REVIEW ARTICLE

Practical pathology of aging mice

Christina Pettan-Brewer and Piper M. Treuting*

Department of Comparative Medicine, University of Washington, Seattle, WA, USA

Old mice will have a subset of lesions as part of the progressive decline in organ function that defines aging. External and palpable lesions will be noted by the research, husbandry, or veterinary staff during testing, cage changing, or physical exams. While these readily observable lesions may cause alarm, not all cause undue distress or are life-threatening. In aging research, mice are maintained until near end of life that, depending on strain and genetic manipulation, can be upwards of 33 months. Aging research has unique welfare issues related to age-related decline, debilitation, fragility, and associated pain of chronic diseases. An effective aging research program includes the collaboration and education of the research, husbandry, and veterinary staff, and of the members of the institution animal care and use committee. This collaborative effort is critical to humanely maintaining older mice and preventing excessive censorship due to non-lethal diseases. Part of the educational process is becoming familiar with how old mice appear clinically, at necropsy and histopathologically. This baseline knowledge is important in making the determination of humane end points, defining health span, contributing causes of death and effects of interventions. The goal of this paper is to introduce investigators to age-associated diseases and lesion patterns in mice from clinical presentation to pathologic assessment. To do so, we present and illustrate the common clinical appearances, necropsy and histopathological lesions seen in subsets of the aging colonies maintained at the University of Washington.

Keywords: *pathology*; *mice*; *aging*; *cancer*; *animal models*; *veterinary pathology*

Received: 16 April 2011; Revised: 10 May 2011; Accepted: 10 May 2011; Published: 1 June 2011

Aging is characterized by progressive declines in multiple organ systems with increases in many neoplastic and chronic degenerative non-neoplastic diseases. Mice are a popular mammalian species for aging studies as they are relatively economical to maintain for long-term aging studies and are similar to humans genetically and physiologically (1, 2). Genetically modified mice (GEMs) have been used extensively to test various hypothesis of aging (3, 4).

While maximum lifespan has been the mainstay metric of aging research, it is recognized that longevity alone, while informative, is incomplete as it does not allow for assessment of health. Physiologic, behavior, and pathology assessment coupled with the foundation of lifespan extension offer a more accurate characterization of a gene or intervention's effect on maintenance of functional health. Pathobiology aging studies are now shifting toward characterizing health span and age-related disease onset in mouse models (5–7).

Defining what constitutes health and therefore health span in mice or humans is not a simple task. Medical experts with years of specialized training in geriatrics and/or biogerontology cannot completely define human healthy aging. For elderly mice, there is no predefined professional curriculum for specialized training, which is comparable to the human track. The mouse 'geriatricians' and biogerontologists are often a team of research scientists, veterinarians, medical doctors, graduate students, veterinary technicians, and animal husbandry staff with varied educational and cultural backgrounds. To find a working consensus of a 'healthy' old mouse is challenging given the diverse backgrounds of the humans working with the mice. It is not a trivial consideration, either. Decisions on treatments and euthanasia for humane reasons are impacted by people's expectations of what is a healthy mouse. Applying a definition proposed in M. Tatar's report on the Biology of Aging Summit (6): 'Good health is recognized by the ability to retain or return to normal levels when a subject is manipulated in a way to perturb a targeted system', is one way to define health in a measureable way. However, 'normal levels' must be predefined, ideally, at the level of the cell, tissue, organ, organism, and colony. Individuals or groups working with the aging mouse colonies must have baseline information from which they can determine what is, and is not, 'normal' for the age of the mouse. If an observer has never seen a 30-month-old mouse, and is only familiar with the appearance of younger mice, they may be apt to classify an old mouse as 'sick' when it actually may only be exhibiting the expected

Citation: Pathobiology of Aging & Age-related Diseases 2011, **1**: 7202 - DOI: 10.3402/pba.v1i0.7202

age-associated frailty and readily observable but non-lethal lesions.

In this paper, we will provide practical overview of old mouse clinical (cage-level) presentations, necropsy, and histological findings in the UW aging mouse colonies. It is designed as an illustrative technical review to provide an introduction to the common disease patterns in older mice. The gross and histologic images are selected to exemplify the common lesions of old mice. It is not intended to be a comprehensive review of strain or gender-specific lesion spectrums. Rather, the aim here is to provide a foundation upon which readers can then build specific knowledge on the nuances of mouse models of aging. Disease spectrums in any one background strain, institution, gender, or genetically modified line (even those with identical background strains and diets) can and do vary (8). The importance of contemporary sex and aged matched wild-type littermate controls derived from the experimental colonies cannot be overstated (9).

Materials and methods

While this is a technical report, detailed methods covering animal housing, pathogen status, and clinical assessments of sick and moribund mice are pertinent as these variables impact phenotypes and vary between facilities. Reporting of such details is in compliance with the ARRIVE guidelines (10). Technical necropsy and histopathology methods are briefly covered for completion; the reader is referred to comprehensive reviews for additional information (11–13).

Animals and husbandry

The mice described herein were obtained from the C57BL/6J (Jackson Laboratories, Bar Harbor, ME) and CB6F1 aged mouse colonies housed at the University of Washington. Additionally, select gross photographs and histopathology examples were obtained from an unrelated inflammatory bowel disease research colony archives (Maggio-Price, University of Washington). In the aging colonies, animals were multiply housed (4–5 per cage, separate sexes) in ventilated cages containing Bed-O-Cob (Andersons, Maumee, OH) in a specific pathogen-free facility at the University of Washington. Mice were fed irradiated Picolab Rodent Diet 20 #5053 (PMI Nutrition International, Brentwood, MO) and provided reverse osmosis water. All supplies entering animal rooms were autoclaved, and rooms were maintained at 70–74°F, 45–55% humidity, with 28 air changes per hour and a 12-hour light/dark cycle. Sentinel mice were tested quarterly and were negative for endo- and ectoparasites, mouse hepatitis virus, mouse parvovirus, and rotavirus, and they were tested annually for *Mycoplasma pulmonis,* pneumonia virus of mice, reovirus-3, Sendai virus, and Theiler's murine encephalomyelitis virus. The mice from aging colonies mice were not tested for Helicobacter species or mouse Norovirus. The housing and experimental protocol for the two Helicobacter-infected mice (Fig. 1C–F) is described elsewhere (14). Historical (1980s) dermatitis and alopecia teaching archival cases presented in Fig. 2C,D lack complete strain and housing history. All animal procedures were approved by the University of Washington Animal Care and Use Committee.

Clinical assessments and definitions of sick versus moribund mice

Clinical observations in mouse colonies typically begin with superficial assessments by the husbandry staff during change changing. These readily conducted assessments include body condition, pelage condition, and activity levels (15, 16). A general consensus for normal mouse appearance includes a well-kept coat, bright eyes, erect ears, active and engaged in its environment (17). If an animal deviates from the observer's definition of normal, it is reported to Veterinary Service Staff through generation of a 'sick animal report'. Veterinary service staff and/or clinicians conduct a thorough physical exam and determine the health status of the mouse. Generally accepted sick rodent signs include hunched posture, unkempt coat, discharge from the eyes or other body orifice, rectal or uterine prolapses, skin lesions, palpable masses, reluctance to move, poor body condition, and/or hydration. The presentation of illness and its severity in a mouse can be varied and therefore descriptive criteria for end points must be established in order to minimize pain and distress and maximize data quality (15). For aging colonies, the mice are ideally maintained until near end of life (EOL) and will have age-associated diseases that may cause some to consider the old mouse 'sick'(18). To prevent unwarranted censoring of mice due to non-terminal diseases, consensus descriptive criteria for end-of-life and humane euthanasia were developed. Mice were considered to be at EOL and euthanized when they were moribund and demonstrated one or more clinical signs suggestive of imminent death within 24 hours (19). These signs included (1) non-responsiveness to being touched, (2) cold body temperature to the touch, (3) slow or labored respiration, (4) hunched body position with matted fur, (5) failure to eat and drink (as determined by food hopper weights and degree of dehydration), or (6) poor body condition score or $>$20% loss of body weight relative to baseline (20). Mice that were nearing EOL, as determined by less severe clinical signs and up to 20% weight loss, were closely examined twice a day, 7 days a week. Mice that met the above criteria were killed by CO_2 and necropsies performed.

Citation: Pathobiology of Aging & Age-related Diseases 2011, **1**: 7202 - DOI: 10.3402/pba.v1i0.7202

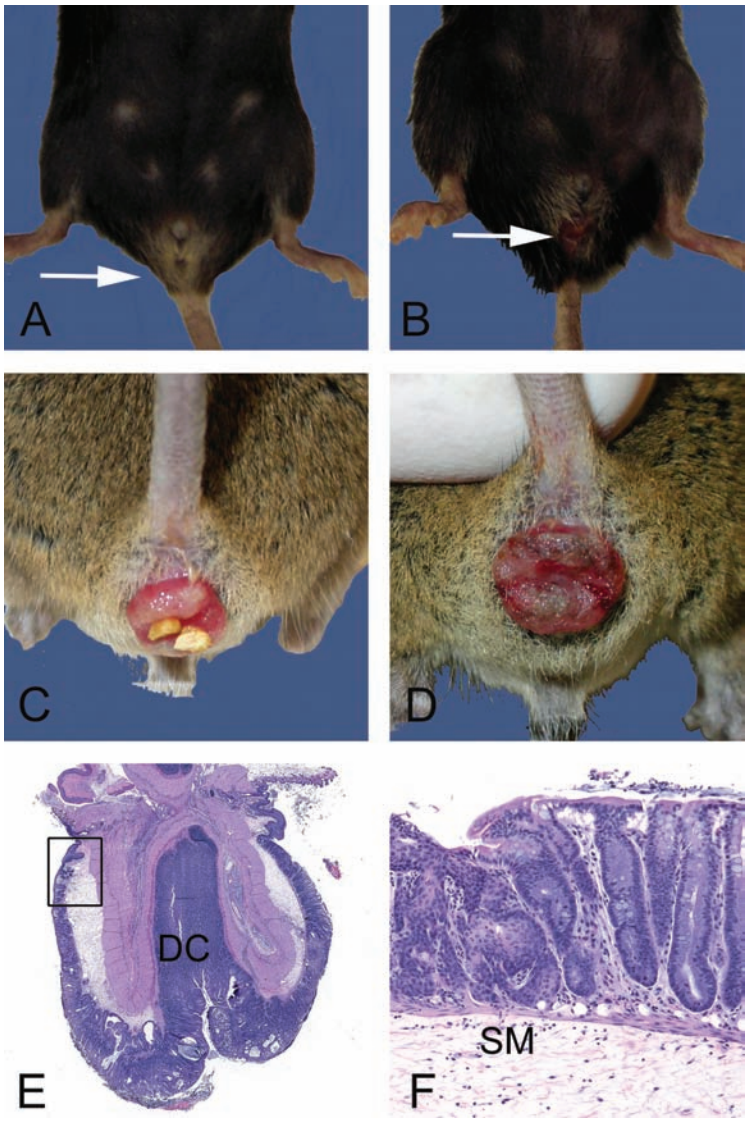

Fig. 1. Gross and microscopic examples of rectal prolapses. **A.** Normal female 28-month-old B6 mouse with the anus indicated (arrow). **B.** Female 28-month-old B6 mouse with a mild acute rectal prolapse. Note the mild protrusion of congested and moist rectal mucosa (arrow). In female mice, rectal prolapse must be differentiated from uterine prolapse. **C.** Moderate to severe subacute rectal prolapse in a 4 to 6-month-old male genetically modified mouse, 129-*Smad3*^{tm1Par}/J, infected with Helicobacter species. **D.** Chronic severe rectal prolapse in a 4 to 6-month-old male *129-Smad3*^{tm1Par}/J infected with Helicobacter species. The mucosa is dry and thickened with adherent crust. **E.** Hematoxylin and eosin-stained section of prolapsed rectum. The prolapsed mucosa is covered by a serocellular crust. Distal colon (DC) and rectoanal junction (box) are indicated. **F.** Higher power of boxed region in E. Squamous metaplasia (arrow) and hyperplasia of the rectal and distal colonic mucosa is common in chronically prolapsed tissues exposed to the cage environment including bedding, skin, and fecal organisms. The submucosa (SM) is markedly expanded by edema.

Necropsy and tissue preparation

At necropsy, of all major organ systems and any grossly abnormal tissues were preserved in 10% neutral phosphate-buffered formalin. Fixed tissues were trimmed using a standard protocol developed by the University of Washington Veterinary Diagnostic Laboratory. Boney tissues were decalcified and all tissues were routinely processed and paraffin embedded. Samples were sectioned at 4–5 μm and stained with hematoxylin and eosin. For the cases described here, up to 30 tissues were examined using a protocol modified after Brayton et al. (12). Histological sections were examined and morphological diagnoses applied by PMT. Lesion definition and severity scoring systems are published elsewhere (21). Neoplastic diagnoses and terminology were based on consensus criteria (22). Special stains were employed in selected cases and included Movat's pentachrome, Masson's trichrome, or periodic acid Schiff's. In some

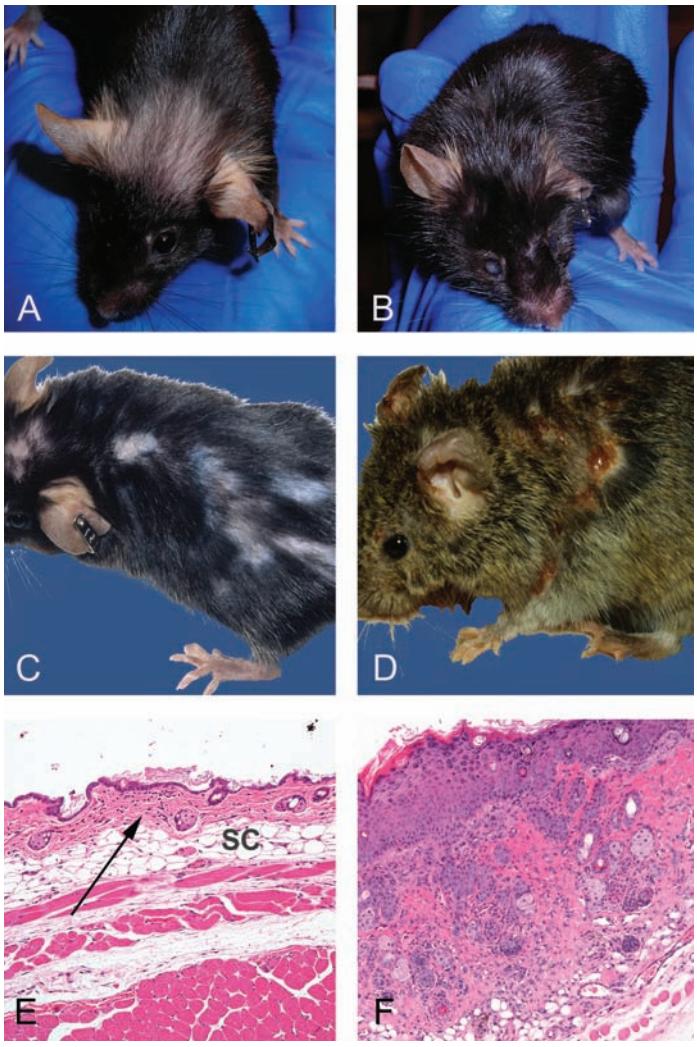

Fig. 2. Clinical and histological presentations of common skin lesions. **A.** A 28–month-old female B6 mouse in relatively good health deemed clinically normal. Note mild alopecia on the head, normal eyes, and well-groomed pelage. **B.** A 28-month-old female B6 mouse with ill-kept fur due to lack of adequate grooming. Note the hunched posture, opaque cornea, the elongated shape of the nose, and relatively boney appearance of this mouse in contrast to the mouse pictured in 2A. Internally, this mouse had a large pituitary adenocarcinoma (see Fig. 5C,D). **C.** Moderate patch alopecia in a B6 mouse (age unknown). This clinical presentation may be a result of dermatitis or alopecia due to other causes such as primary follicular dysplasia. Histology would aid in determining a definitive cause. **D.** Ulcerative and likely pruritic dermatitis in an agouti mouse (background and age unknown). This historical clinical presentation was often seen associated with fur mites, although numerous causes have been implicated in a similar clinical spectrum in C57BL/6 mice. See text for details. **E.** Hematoxylin and eosin-stained section of mild alopecia with minimal chronic inflammation within the dermis (arrow). Note thickness of the subcutis (SC). Follicles are sparse and devoid of hair shafts. **F.** Hematoxylin and eosin-stained section of severe proliferative dermatitis (pseudoepitheliomatous). The epidermis is markedly thickened with irregular rete peg formation in this somewhat tangentially oriented section. Dyskeratosis and mild orthokeratotic hyperkeratosis are also present with moderate chronic dermatitis that extends into the SC. Pseudoepitheliomatous hyperplasia is frequently seen histologically at the thickened edges of chronic ulcerative foci (see 2D).

cases, complete blood counts with differentials and clinical chemistry were analyzed on blood obtained from the heart at necropsy (Phoenix Central Laboratories, Everett, WA).

Review of pathology reports and databases

Numbers of specific neoplastic and non-neoplastic diagnoses in aging B6 mice were determined by review of individual histopathology reports and databases. Non-neoplastic lesions were counted and tabulated by disease processes regardless of lesion severity. Prevalence was calculated as the number of mice affected. Table 1 has the numbers of mice with the histologic neoplastic diagnosis. Table 2 lists the non-neoplastic disease diagnosed either at cage level, necropsy, and/or histologically. Results were tabulated with sexes combined except where noted. A

Citation: Pathobiology of Aging & Age-related Diseases 2011, **1**: 7202 - DOI: 10.3402/pba.v1i0.7202

Table 1. Survey of aged C57BL/6J colony neoplastic disease spectrum

Neoplastic diseases	Location	% of mice with
Fibrosarcoma	Uterus, skin, perirenal, ear	4
Hemangioma	Spleen	1
Hemangiosarcoma	Spleen, uterus, ovary, liver, skin	4
Hematopoietic neoplasia (Malignant lymphoma or Histiocytic sarcoma)	Systemic	67
Hepatic adenoma	Liver	1
Leiomyosarcoma	Seminal vesicle, colon	3
Malignant Pheochromocytoma	Adrenal	1
Osteosarcoma	Vertebra	1
Ovarian granulosa cell tumor	Ovary	1
Pituitary adenocarcinoma	Pituitary	1
Pituitary adenoma	Pituitary	6
Pulmonary adenocarcinoma	Lung	3
Pulmonary adenoma	Lung	1
Squamous cell carcinoma	Skin	1
Squamous papilloma	Stomach	3
Testicular interstitial cell adenoma	Testicle	1

Note: Retrospective review of clinical data, necropsy, and histology findings was tabulated. Results reported as percentage of mice with the disease ($n = 72$; males = 26, females = 46). Age range 16–36 months.

comprehensive review of gender-specific lesion spectrums in a number of inbred strains, including UW aged C57BL6, will be published elsewhere. Compete blood counts with differentials and clinical chemistry panels for two of the mice are presented in Table 3.

Results and discussion

Aging mice housed at the UW have four common clinical presentations, which are readily observable at the cage level and thus are frequently reported. These include rectal prolapse, alopecia and dermatitis, ocular lesions, and palpable masses. Whereas mice are reported and sometimes euthanized due to one of the above disease processes, there are often unsuspected comorbidities that may be more severe than the initial presenting clinical diagnosis. Many pathophysiological processes associated with aging, such as tissue atrophy, chronic inflammation, dysplasia, and occult neoplasia may not result in robust clinical signs (18). Additionally, moribund animals may be euthanized due to relatively non-specific signs such as hunched, cold to the touch with loss of body condition, and increased respiratory effort. The morbid state is often

Table 2. Survey of aged mouse colony non-neoplastic disease spectrum in C57BL/6J mice housed at the University of Washington

Non-neoplastic diseases	Location	% of mice with
Acidophilic macrophage pneumonia	Lungs	13
Amyloid, glomerular	Kidney	41
Amyloid, intestinal	Small intestine	14
Biliary hyperplasia	Liver	3
Cataracts or cornea opacity	Eyes	30
Chronic infarct	Kidney	4
Cystic endometrial hyperplasia	Uterus	14
Heart lesions[a]	Heart	97
Hepatic cysts	Liver	3
Hydronephrosis[b]	Kidney	19
Nephropathy	Kidney	100
Ovarian atrophy	Ovary	6
Ovarian cysts	Ovary	3
Polyarteritis	Systemic arteries	10
Preputial cystic adenitis	Preputial glands	3
Rectal prolapse[b]	Rectum	19[c]
Seminal vesiculitis, cystic degeneration	Seminal vesicles	17
Skin lesions[d]	Skin	17
Systemic antigenic stimulation	Most major organs	60
Testicular degeneration	Testes	19
Ulcerative keratitis	Eyes	13

Note: Retrospective review of clinical data, necropsy, and histology findings was tabulated. Results reported as percentage of mice with the disease regardless of severity with a range of minimal to severe ($n = 72$; males = 26, females = 46). Age range 16–36 months.

[a]Includes cardiomegaly, cardiomyopathy, arteriosclerosis, valvular lesions, and amyloidosis.

[b]Diagnosed at cage level or at necropsy.

[c]Out of total colony, $n = 711$.

[d]Includes dermatitis and alopecia.

a result of the combination of diseases, especially in older mice (21, 23). To characterize the full spectrum of lesions present at the EOL, and the definitive diagnosis of diseases, necropsies and histological examinations are required. Whereas clinical pathology including complete blood counts with differentials and chemistry panels are widely used antemortem diagnostic tests in most species, the limited amount of blood that can be humanely obtained from live mice restricts the number of tests that can be performed with any one sample. However, terminal blood collection usually provides an adequate

Table 3. Clinicopathological data from B6 mouse presented in Figures 2B, 5C, and 5D and CB6F1 mouse presented in 3B, 3D, and 4C

	B6 Female Figs. 2B and 5C,D	CB6F1 Male Figs. 3B,D and 4C	Reference values[a]
Complete blood count			
WBC, K/ul	2.5	14.8	5.1–11.6
RBC, M/ul	8.5	11.1	8.7–10.5
HGB, g/dl	12.9	15.4	12.2–16.2
HCT,%	51.0	55.8	42–44
MCV, fl	60.1	50.1	na
MCH, pg	15.3	13.8	na
MCHC	0.3	27.6	na
Platelet count, K/ul	992.0	2043.0	100–1,000
Differential			
	Absolute/μl (%)	Absolute/μl (%)	
Bands	0 (0.0)	0 (0.0)	0
Polys	960 (38.0)	6,220 (42.0)	6.7–37.2
Lymph	1,240 (49.0)	7,090 (48.0)	63–75
Monos	250 (10.0)	1,030 (7.0)	0.7–2.6
Eos	80 (3.0)	440 (3.0)	0.9–3.8
Baso	0 (0.0)	0 (0.0)	0–1.5
Comments	Polychromasia, +1	Slight polychromasia Platelet count inaccurate due to clumps	
Small mammal panel			
Glucose mg/dl	196.0	170.0	106–278
Urea nitrogen (BUN), mg/dl	24.0	30.0	19–34
Calcium, mg/dl	10.6	10.1	9–12
Total protein, g/dl	6.9	5.7	4.3–6.4
Albumin, g/dl	3.5	3.2	2.0–4.7
Alanine aminotransferase, U/l	43.0	47.0	26–120
Aspartate aminotransferase, U/l	83.0	107.0	69–191
Principal histologic diagnoses	Pituitary adenocarcinoma Histiocytic sarcoma Keratitis and corneal ulceration Polyarteritis	Harderian gland adenoma Preputial adenitis and seminal vesiculitis Mild nephropathy	

[a]Summarized from (58, 59).

volume for full panels. Table 3 provides clinical pathology data and histopathological diagnoses for two of the mice illustrated in this manuscript. In the mice presented here, renal, vascular, inflammatory, and degenerative diseases were the common lesions diagnosed by histology. In the following section, the common age-associated diseases and lesions in the C57BL/6J colony at the UW are reviewed and illustrated.

Rectal prolapse

The mouse rectum, in contrast to the human, is extremely short and is susceptible to prolapse. Rectal prolapse (Fig. 1) in mice may be caused by inflammation in the colon due to infectious agents, such as pinworms or Helicobacter species (Fig. 1C–F), with increased abdominal pressure caused by pregnancy, masses, stranguria, or diarrhea. With age, it is plausible that the pelvic musculature may weaken allowing for prolapses to occur more readily – although this has not been investigated extensively (24). In many cases, the definitive cause for rectal prolapse is not determined; however, known causes may be excluded. In the UW aging colonies, pinworms and *Citrobacter rodentium* have not been diagnosed. The colonies are not tested for Helicobacter species, which can cause colitis and rectal prolapse in certain susceptible GEMs such as the 129-*Smad3*^{tm1Par}/J model of bacterial-driven colon cancer (14). In immune competent mice, such as B6, Helicobacter species are considered commensal and should not cause disease. Rectal prolapses vary in clinical appearance (Fig. 1B–D) and, in female mice, must be distinguished from uterine or vaginal prolapse. Mild prolapse is a protrusion of the rectum extending only 1–2

Citation: Pathobiology of Aging & Age-related Diseases 2011, **1**: 7202 - DOI: 10.3402/pba.v1i0.7202

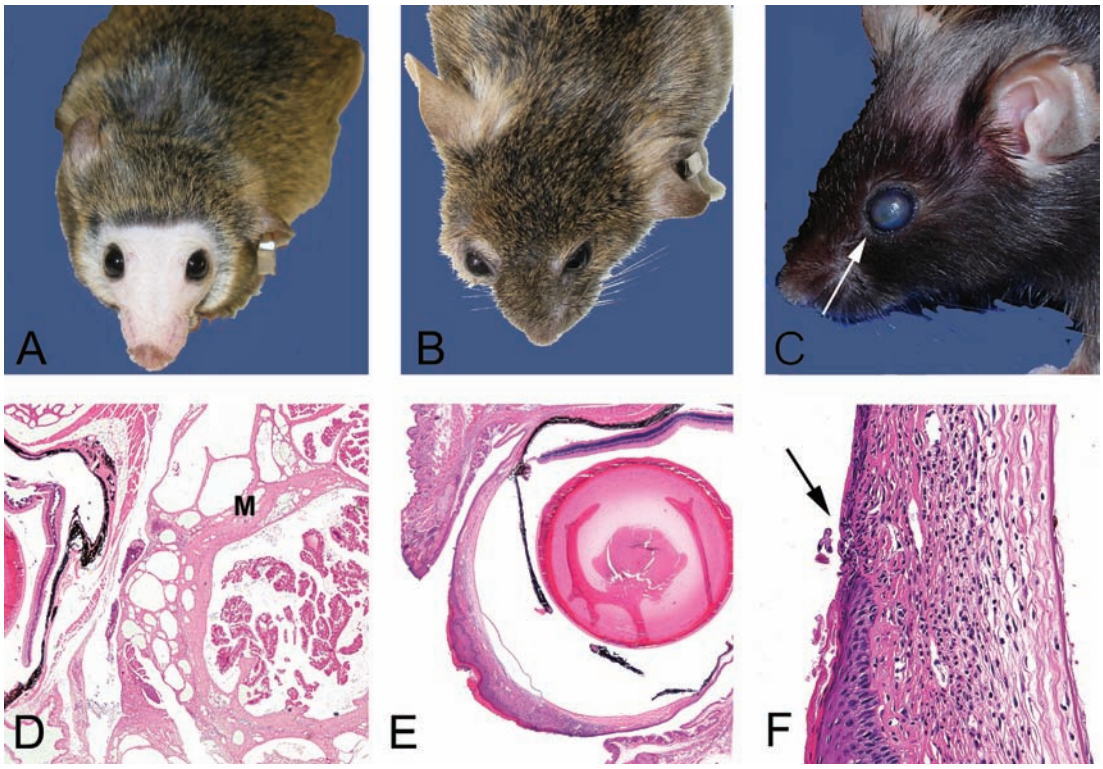

Fig. 3. Clinical and histological presentations of common eye lesions. **A.** Normal periocular shape, eye size, and color in a 24-month-old CB6F1 mouse included here for contrast to the mouse in 3B. Note the lack of pelage and vibrissae due to extensive barbering by cage mates. Barbering is another relatively common skin presentation. It may lead to dermatitis in the victim and impaction of hair fragments into gingival sulcus of the barber. **B.** A 24-month-old CB6F1 mouse has periocular and retrobulbar swelling (between arrows) with bulopthalmia. This presentation may be a result of periocular cellulitis, conjunctivitis, or retrobulbar mass such as an abscesses or neoplasia. In this mouse, the swelling was due to a large retrobulbar mass (4C), which was diagnosed histologically as a Harderian adenoma (3D) **C.** Corneal opacity in a 28–month-old B6 mouse. The small foci (arrow) at the rostal aspect of the cornea is an ulcer, which was confirmed clinically with fluorescein dye test clinically and histologically (3F) **D.** Hematoxylin and eosin-stained section of the Harderian gland adenoma from the CB6F1 mouse in panel 3B. The mutliobulated and expansible mass (M) is located in the retro-orbital space compresses the eye (E). **E.** Hematoxylin and eosin-stained section of the eye from the B6 mouse in 3C. The opacity noted clinically is due to marked proliferative and ulcerative keratitis (box). The normal corneal epithelium is non-keratinized and 4–7 cell layers thick. **F.** Higher magnification of boxed region of a punctate corneal ulcer in 3C and E. The defect in the overlying corneal epithelium (arrow) exposes the stroma. The hydrophilic stroma will uptake fluorescein dye when the hydrophobic epithelial layer is breeched. Note the dense inflammatory infiltrate and neovascularization in the stroma. These also contribute to the corneal opacity noted clinically (3C).

mm from the base of the tail and perineum and the prolapsed mucosa is light pink and moist, with little adherent material (Fig. 1B). Mild prolapse often cause little detriment to the animal, which can survive and thrive with these lesions for some time. Severe rectal prolapse is a protrusion of both distal colon (DC) and rectal mucosa extending >3 mm from the base of the tail and perineum (Fig. 1C,D). The severely prolapsed mucosa is often reddened and edematous to necrotic with adhered fecal or bedding material (Fig. 1C). Often, feces inside the cage will be sticky, an indication of diarrhea. In long-standing cases, the mucosa may become proliferative (Fig. 1D). Exposure of the delicate colorectal mucosa to the cage environment provides a nidus of chronic inflammation and entry of bacteria in the systemic circulation. There is no completely effective treatment for rectal prolapse. Clinical recommendations for mice with rectal prolapses vary between facilities and experimental protocols; in general, mild rectal prolapses with no other clinical signs of systemic illness are often monitored, while euthanasia is recommended for mice with moderate to severe rectal prolapses.

Histologically, the prolapsed mucosa may be ulcerated to necrotic or, with chronicity, proliferative with squamous metaplasia (Fig. 1E,F). Adherent bacterial colonies, plant material and fecal matter may also be present. In typical cases, the underlying vasculature and submucosa (SM) is edematous and inflamed and may be congested. Inflammation may be acute, primarily neutrophilic when there are ulcers and bacteria, or lympho-

histiocytic when chronic. Chronic prolapse can lead to severe mucosal hyperplasia with subsequent mucosal herniation due to the thin SM. The herniated glands must be differentiated from invasive carcinoma (25).

Skin lesions

Barbering, alopecia, dermatitis, and scarring are commonly seen in mice (Fig. 2). Dermatitis may have a variety of causes including infectious agents, such as fur mites, or fighting with secondary bacterial infections. These will often respond to treatments such as removal of aggressive mice, topic and oral antibiotic, or corticosteroids (26). In contrast, idiopathic ulcerative dermatitis in the B6 mouse does not respond to treatment. Affected B6 mice are usually pruritic leading to self-mutilation, disease progression and, often, euthanasia for humane

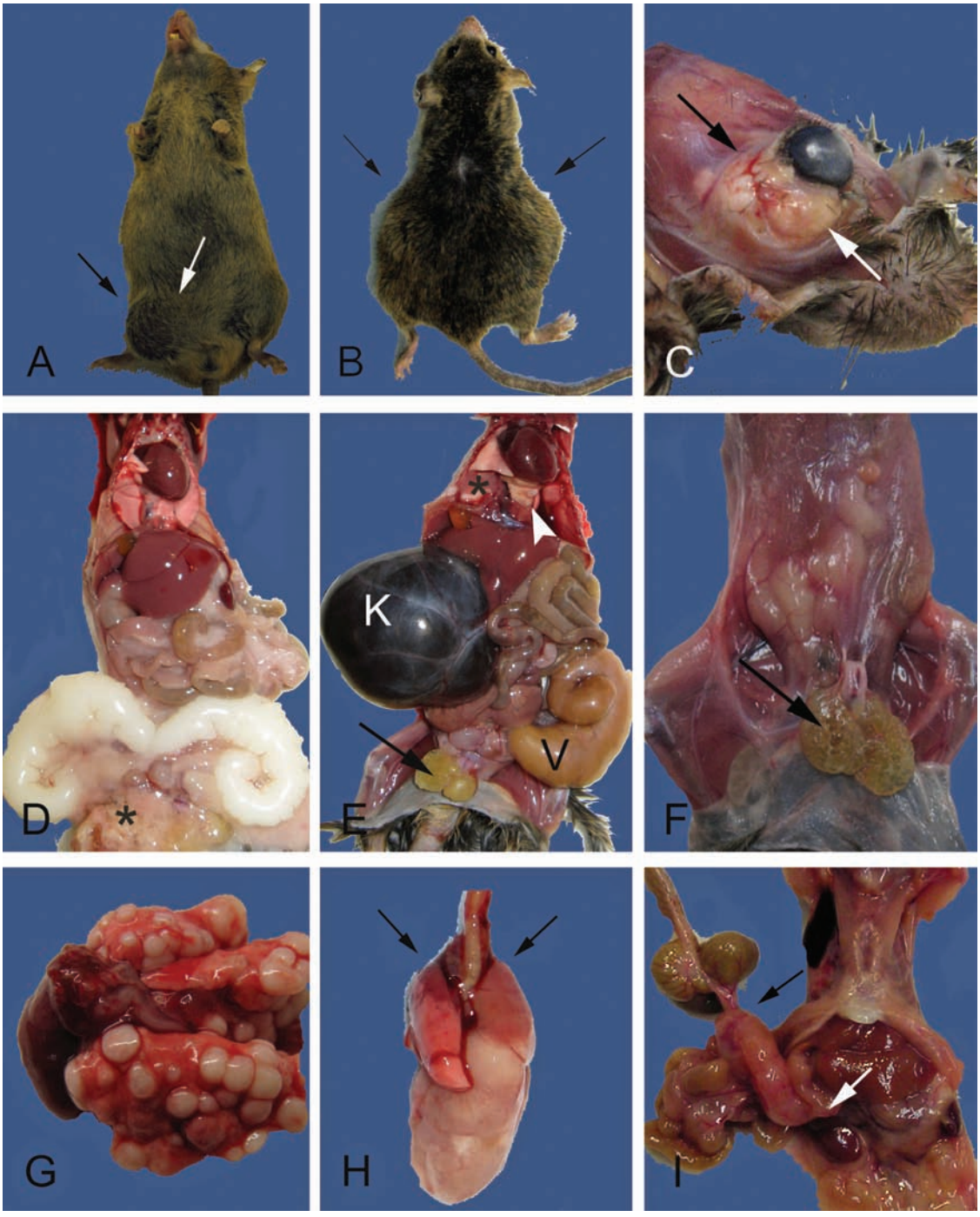

Fig. 4 (*Continued*)

Citation: Pathobiology of Aging & Age-related Diseases 2011, **1**: 7202 - DOI: 10.3402/pba.v1i0.7202

reasons. The B6 chronic ulcerative dermatitis has been attributed to many causes (27, 28) most recently primary follicular dystrophy (29). The clinical disease is variable, waxes and wanes, appears to have sex, and season predilections. As seen with other strain-specific diseases, the use of F1 hybrids has a decreased incidence of B6 dermatitis (1, 30); however, skin lesions remain a significant background factor in aging colonies (29). Collectively, skin lesions in aging mouse colonies have variable presentations ranging from the very mild alopecia to severe ulcerative disease requiring euthanasia. Mild changes, such as ill-kept fur (Fig. 2B) are often one of the first clinical signs noted in diseased mice. It is non-specific and a result of decreased grooming. Alopecia in mice may present on the head (Fig. 2A) or in a patches (Fig. 2C). Barbering by cage mates may result in areas of hair loss; however, distinctive patterns (Fig. 3A) and the presence of one unaffected (dominant) mouse in the cage will help to rule out dermatitis. Histologically, dermatitis is also variable in presentation and severity, depending on etiology and chronicity. Mild lesions (Fig. 2E) with few scattered inflammatory cells may be noted in regions of clinical alopecia. Severe lesions may occur and are often a combination of ulceration, necrosis, and associated chronic-active inflammation. Healing is by dermal fibrosis and marked epithelial hyperplasia (Fig. 2F). Like rectal prolapses, open skin lesions serve as a nidus for bacterial infection with skin commensals (Staphylococcal species) and result in smoldering inflammation that may affect physiological parameters such as inflammatory cytokines, leukograms, lymphadenopathy, and reactive amyloidosis (31).

Ocular lesions

The cornea of mice is relatively large compared to humans and is exposed to exogenous irritants such as bedding dust and ammonia levels, which can cause contact keratitis. Skin commensals may also contribute to keratitis, conjunctivitis, and blepharitis. With age, atrophy and chronic inflammation of the lacrimal glands is very common and may result in decreased tear production and secondary corneal lesions (*keratoconjunctivits sicca*). Regardless of the cause, cornea lesions present as opaque eyes with variable amount of discharge. In pigmented strains, corneal opacity is particularly easy to recognize due to the contrast with the dark globe (Fig. 3C). Ulcerative keratitis may be diagnosed clinically via ophthalmic exams and fluorescein stain uptake into the ulcerated cornea. Treatment options may include antibiotics and or steroids and will vary by facility and experimental protocol. Frequently in aged mice, the bulk of the ulceration and active inflammation is resolved; histologically, the chronic corneal lesion is characterized by proliferation of the corneal epithelium with varying neovascularization and chronic inflammation (Fig. 3E,F). Other eye lesions commonly reported include proptosis with or without bulopthalmia secondary to retrobulbar abscesses, Harderian gland, or intraorbital gland neoplasias (Fig. 3B,D). Cataracts are also quite common in aged mice but are more challenging to diagnose clinically usually requiring slit lamp examination (32, 33) antemortem or postmortem histopathological assessment.

Palpable masses

Subcutaneous or internal palpable masses may be due to neoplasia or abscesses, possibly both, and are common in aged animals. Affected mice present with irregular body contours and may have decreased mobility if the masses are large or in the inguinal or axillary areas (Fig. 4A,B). In the UW aging colonies, enlarged and occasionally infected seminal vesicles in male mice were reported

Fig. 4. External and internal masses may be due to degenerative, inflammatory, or neoplastic lesions. **A.** Swelling in the lower right abdomen and the inguinal region (between arrows) are present in this 24-month-old male CB6F1. The inguinal swelling is due to an infected preputial gland. The abdominal swelling is due to enlarged, but otherwise normal, seminal vesicles (see also D). **B.** A 27-month-old male CB6F1 with bilateral abdominal swelling (arrows) from severe unilateral hydronephrosis and enlarged and infected seminal vesicles (see also E). **C.** A large multilobulated retro-orbital mass causing proptosis of the eye (between arrows). The cornea is cloudy due to keratitis (see also Fig. 3B,D). **D.** Internal examination of the mouse in A demonstrates bilaterally enlarged seminal vesicles, a common finding in older male mice. The seminal vesicular fluid is normally white and will discolor with infection or infarction (compare to E). Additional gross lesions are an enlarged heart with mild hepatomegaly, pneumonopathy, and the preputial abscessation (*) noted in A (between arrows). **E.** The internal examination of the mouse in B demonstrates severe unilateral hydronephrosis (K) and enlarged and infected seminal vesicle (V). The kidney is filled with dark brown colored fluid, a severe sequelae of obstructive uropathy (mouse urologic syndrome). Other lesions include absence of body fat, enlarged and cystic preputial glands (arrow), enlarged heart and pulmonary atelectasis (*), and light yellow firm foci (arrowhead) diagnosed histologically as AMP (see Fig. 6K,L). **F.** A 29-month-old male CB6F1 with bilateral cystic preputial glands (arrow), scant body fat (body condition score of 2/5), and tacky appearing tissues (mild to moderate dehydration). **G.** Multiple pulmonary neoplastic foci in a 30-month-old female CB6F1 mouse. This unusual presentation is more consistent with metastatic rather than primary disease. Histopathological diagnosis, however, confirmed mucinous pulmonary adenocarcinoma (see inset Fig. 5B). **H.** Typical presentation of a CB6F1 pulmonary adenocarcinoma from 28 to 30-month-old mice. Grossly, one large white firm mass extends from the right lung. Microscopically, there may be multiple foci of neoplasia. Cranioventral atelectasis and consolidation of the lungs is also present (arrows). **I.** A large mesenteric mass in the region of a cluster of lymph nodes (bracketed by arrows) from a 28-month-old B6 mouse. Differentials include lymphoma and histiocytic sarcoma. Hepatic involvement with the neoplastic process is suggested by the roughened appearance of the liver (compare to D and E) and was confirmed histologically.

initially as abdominal tumors (Fig. 4A,B). In older B6 male mice, progressive enlargement of the seminal vesicles is extremely common (34) and our experience suggests that it is also common in CB6F1 hybrids. Subcutaneous masses in the inguinal or pelvic region often were enlarged cystic or infected preputial or clitoral glands (Fig. 4E,F). The subcutaneous lymph nodes, especially the submandibular, may be enlarged due to

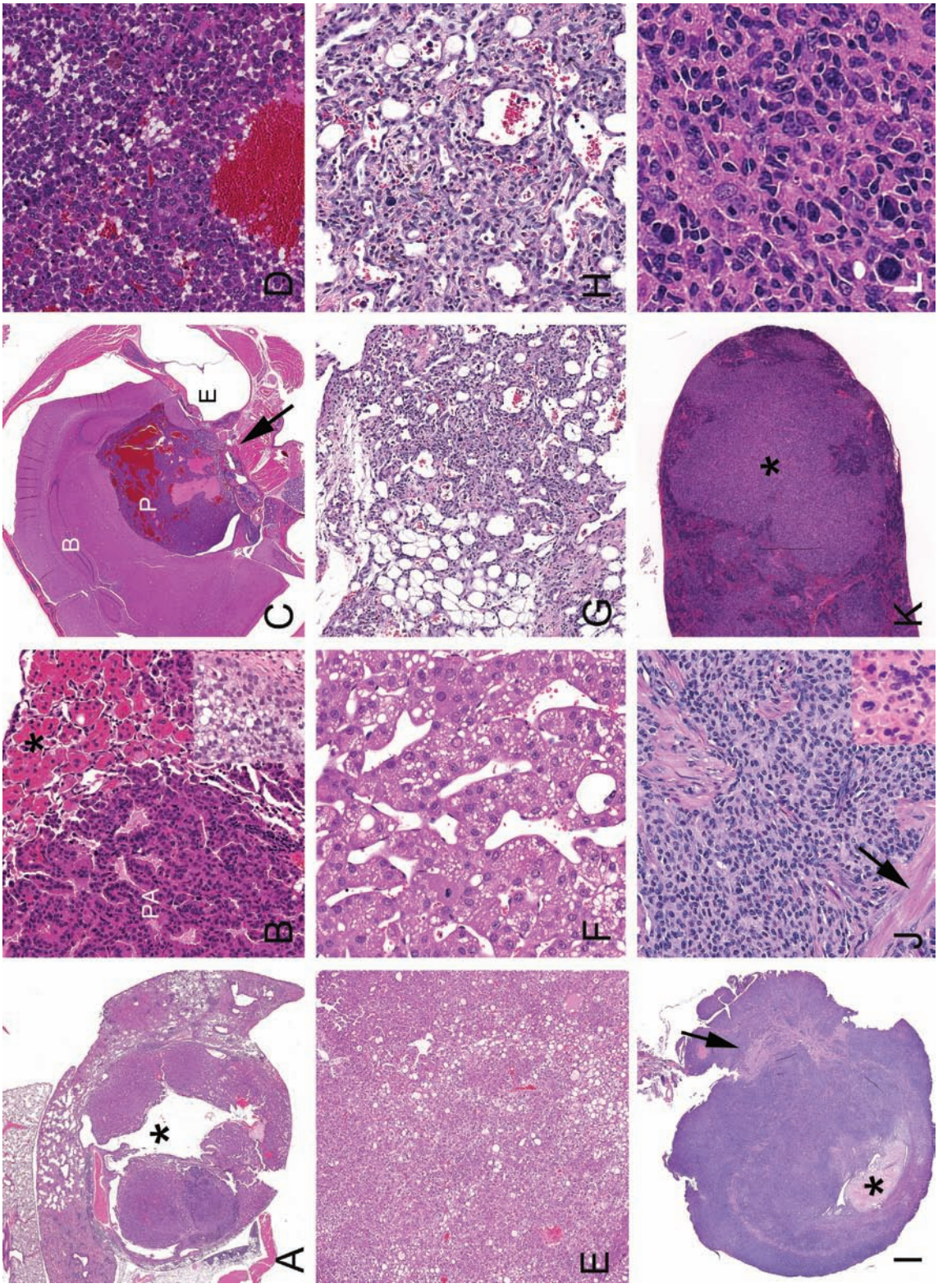

Fig. 5 (*Continued*)

Citation: Pathobiology of Aging & Age-related Diseases 2011, **1**: 7202 - DOI: 10.3402/pba.v1i0.7202

physiologic lymphoid reactive hyperplasia secondary to systemic or localized inflammation. Systemic lymphadenopathy involving subcutaneous and internal lymph nodes is most frequently due to malignant lymphoma. Other subcutaneous structures such as the mammary fat pads or salivary glands may also become inflamed or neoplastic and present as palpable masses. Often, the masses can be diagnosed as inflammatory or neoplastic at necropsy with the combination of the gross presentation and cytology. However, histopathology is definitive as neoplasia may also be infected or inflamed. For example, the retro-orbital mass in Fig. 4C was suspected clinically, and at necropsy, to be a chronic retrobulbar abscess. Final histopathological diagnosis was a Harderian gland adenoma (Fig. 3D). For malignancies within the lung, determining whether neoplastic masses are primary lung tumors versus metastatic disease may be challenging without the aid of histology (Fig. 4G,H). Inbred strains vary in their typical spectrum of disease and neoplasia is no exception (9, 35, 36). In the B6 background, hematopoietic neoplasias (malignant lymphoma and histiocytic sarcoma) are extremely common (Table 1) (21, 36, 37). Necropsy findings for these hematopoietic neoplasias often overlap, for example, enlarged mesenteric lymph nodes (Fig. 4I) can be affected by either type. While there are differences in organ distribution and cellular morphology (Fig. 5I–L) that allow distinction between the malignant lymphomas and histiocytic sarcoma, definitive diagnosis may require immunohistochemical or molecular analysis (38–40).

Lesions diagnosed at necropsy or histologically

Frequently, internal lesions not detected at physical exam, will be observable at necropsy. For example, in a mouse with labored respiration, the lungs may contain pulmonary tumors with an enlarged heart (Fig. 4G, H). A mouse reported with head tilt or circling may be submitted to necropsy to rule out central nervous system disease, but is more likely to have otitis media/interna or arteritis impacting the vestibular system (31). Neurological signs may be due to compression of brain tissue by intracranial neoplasias such as pituitary adenoma/adenocarcinoma (Fig. 5C,D). Splenomegaly is a frequent non-specific necropsy finding that can be due to extensive extramedullary hematopoiesis, which occurs as a physiological response to stimuli such as chronic inflammation or neoplastic diseases (31). With either cause, the spleen can be markedly enlarged (41). Histology can aid in definitive diagnosis of gross lesions that have multiple differential diagnoses.

Complete histopathological examination often reveals more disease processes than were suspected clinically or diagnosed at necropsy. These microscopic morphological data offer insight into unexpectedly interesting or confounding covariates. Necropsy and pathology also serves to confirm the absence of excluded agents, for example, internal and external parasites or evidence of mouse coronavirus (mouse hepatitis virus). Table 2 summaries the microscopic non-neoplastic diagnoses and histological examples are presented in Fig. 6 and Fig. 7. Common non-neoplastic diseases diagnosed histologically include renal disease, arteritis, systemic inflammation, and degenerative lesions.

Renal disease

Renal lesions are common in older mice and include chronic nephropathy, glomerular amyloidosis (42), glomerulonephropathies (43), and obstructive uropathy (44). Kidneys with chronic nephropathy and or glomerular amyloid (if severe) appear pale and pitted and the size may be altered. Cysts, infarcts, and hydronephrosis all may impact kidney size and shape. Obstructive uropathy is common in male mice and is due to blockage of the lower urinary tract from multiple causes (44). Retention of urine may result in or from inflammation of the urogenital tract or accessory sex glands and pressure may cause hydronephrosis (Fig. 4E). Histologically, chronic nephropathy is characterized by early tubular lesions and progresses to include glomerular changes and interstitial inflammation (Fig. 6C,D). There is a large reserve capacity of the kidney to maintain function even in the face of nephron loss thus, for nephropathy alone to cause significant morbidity, it would have to be moderate to severe or accompanied by other lesions affecting the

Fig. 5. Histological presentations of neoplasia. **A.** Pulmonary adenocarcinoma with gross presentation similar to the mouse in 4H. Note large cystic space (*). **B.** Higher magnification of a pulmonary adenoma (PA) with associated AMP (*). Inset: Mucinous pulmonary adenocarcinoma from lungs pictures in Fig. 4G. **C**. Decalcified cross-section of the head with a pituitary adenocarcinoma (P) of the pars distalis from mouse pictured in 2B. Pars distalis tumors typically are hemorrhagic and develop blood filled cystic spaces. Malignancy, in this case, was evident with invasion into the sphenoid bone (arrow). Brain (B), pituitary tumor (P) and ear (E) are indicated. **D.** Higher magnification of the pituitary adenocarcinoma in C. **E.** Liver with solid and trabecular hepatocellular carcinoma (HCC) from a 30-month-old female CB6F1. **F.** Higher magnification of trabecular HCC. **G.** Dermal hemangiosarcoma from a 30-month-old male CB6F1. H. Higher magnification of G. Irregular vascular channels are formed by atypical and anisokaryotic endothelial cells. **I.** Uterus from a 28-month-old B6 mouse is effaced with histiocytic sarcoma (HSA). Broad ligament (arrow) and formed lumen (*) are indicated. **J.** Higher magnification of HSA in I. Neoplastic histiocytes may have elongated oval to round nuclei or form multinucleated giant cells (inset). Myometrial smooth muscle (arrow) is indicated. **K.** Spleen with pleomorphic/follicular malignant lymphoma (*) from a 30-month-old CB6F1 female. **L.** Higher magnification of K. Pleomorphic lymphoma can resemble HSA. Anatomic distribution, morphology, and immunohistochemistry can aid in differentiation.

kidney such as hydronephrosis or neoplasia. However, subclinical or mild nephropathy with associated diminished renal reserve would increase susceptibility to additional insults and homeostatic imbalance (45). Glomerular amyloidosis and membranous glomerulonephropathy may appear histologically similar and can be differentiated by use of Congo Red for amyloid and PAS for increased mesangial matrix (31).

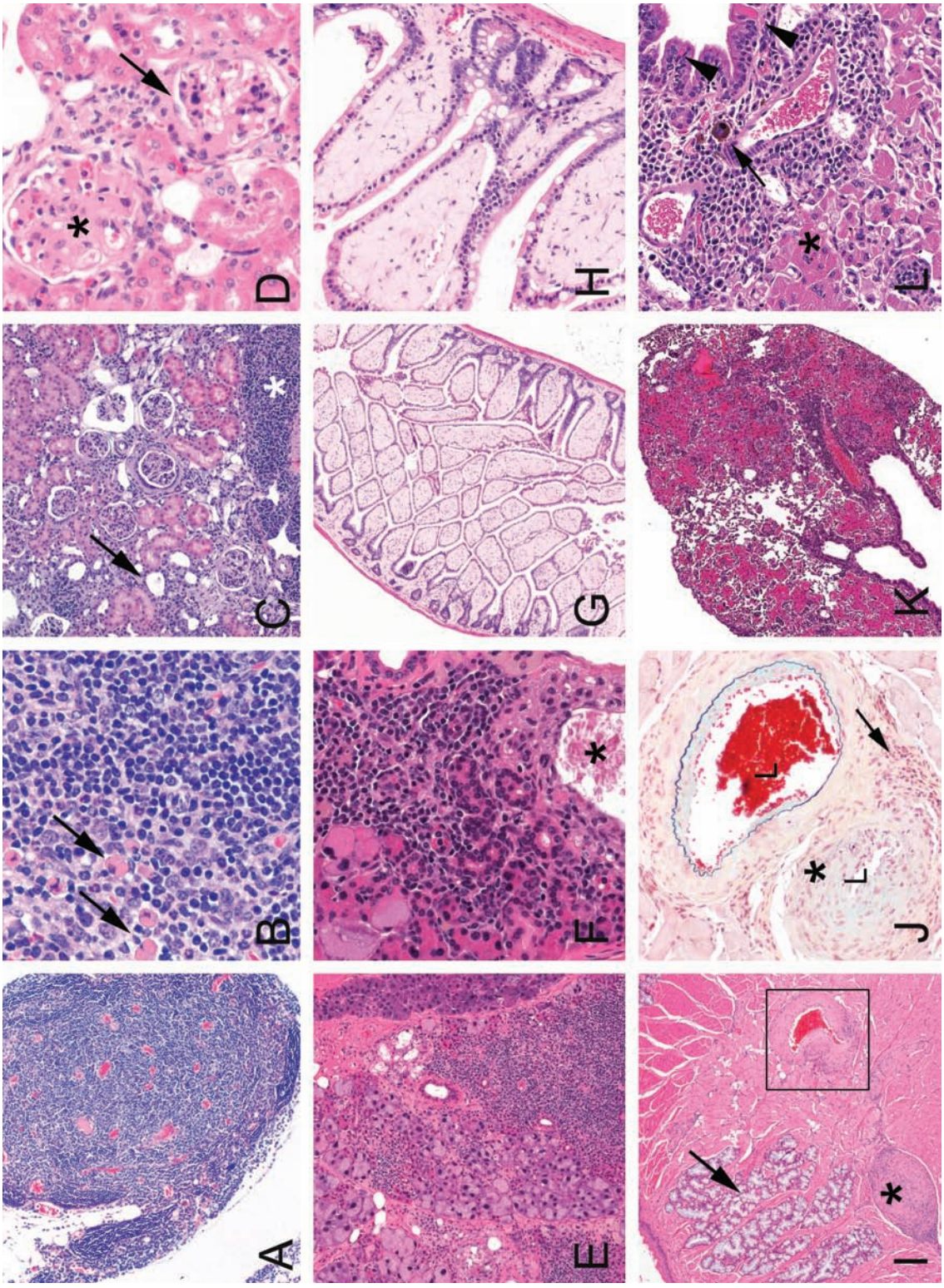

Fig. 6 (*Continued*)

Citation: Pathobiology of Aging & Age-related Diseases 2011, **1**: 7202 - DOI: 10.3402/pba.v1i0.7202

Arteritis

Segmental arteritis with variable components including fibrinoid necrosis, smooth muscle proliferation, and mixed inflammation occurs in small to medium arteries of various organs (Fig. 6I,J) (31). Commonly affected tissues in these studies included the mesentery, tongue heart, reproductive tracts, and kidney. An immune mediate pathogenesis has been proposed (27, 46). In humans with a similar disease processes, polyarteritis nodosa, clinical signs are related to affected organ dysfunction (47). In mice, the most overt clinical sign associated with arteritis is vestibular syndrome (head tilts and/or circling) as describe above (31).

Chronic inflammation

As a secondary process of many diseases associated with aging in mice, and consistent with reports of a proinflammatory state in elderly humans (48, 49) and mice (19), histologic evidence of systemic immune stimulation is present in numerous tissues. Findings include reactive lymphoid hyperplasia in spleen and lymph nodes, increased lymphoid aggregates in various organs, expansion of mesenteric/omental milk spots, acidophilic macrophage pneumonia (AMP), reactive amyloidosis, and the renal lesions discussed above. Omental milky spots (50), mesenteric aggregates with mixed lymphocytes, histiocytes, and plasma cells are frequently reactive in older mice with germinal centers and occasional Mott cells (Fig. 6A,B). Similar reactive changes can be present in lymphoid aggregates found in various tissues including the renal pelvis, bladder, lungs, and liver. Reactive lymph nodes may present clinically as a lymphadenopathy with histological sinusoidal histiocytosis, mastocytosis, or plasmacytosis with germinal centers, which aid in differentiating hyperplasia from neoplasia. AMP is a common idiopathic disease in mice, especially of those on B6 and 129Sv background (51, 52). Although definitively diagnosed with histopathology, severe AMP may be noticed at necropsy as foci of firm, pale tan to cream areas in the lungs, which fail to collapse. The AMP is often associated with pulmonary neoplasia (Fig. 5A,B) or chronic pneumonia (Fig. 6K,L) (31, 53). The characteristic histopathologic lesion is accumulations of large macrophages with abundant cytoplasm containing variable numbers of bright eosinophilic crystals. Multinucleated giant cells, epithelial hyalinosis, and extracellular acicular crystals may also be present (51).

Miscellaneous degenerative lesions

Dysplastic and degenerative dental and joint lesions are presented in Fig. 7 as examples of subclinical histologic disease, which likely contributes significantly to the decline in functional health of the affected mouse and may be under diagnosed. We and others (54) have noted dysplastic intrapulpal denticles in the incisors of older mice (Fig. 7A,B). These lesions may result in abnormal wear and or breakage of the incisors that contribute to periodontitis and decreased ability to effectively gnaw rodent chow. We have noted, in two of three cases of intrapulpal denticles, an association with moderate to severe temporomandibular osteoarthritis (Fig. 7C,D). The precise relationship between the development of these two lesions is unknown – whether the abnormal tooth development aggravated the joint disease or vice versa. It is plausible that the combination of the lesions results in painful and ineffective mastication. Osteoarthritis of the knee, hip, elbow, and vertebra would result in abnormal gaits and, if severe, clinically recognizable joint swelling due ossification of the joint capsule and periarticular fibrosis (55). Preliminary necropsy results from the current health span study in CB6F1 suggest the incidence of clinical osteoarthritis may be relatively high (personal observation CPB). Other preliminary observations from necropsies in the on-going health span study include high incidence of skin, male reproductive tract, renal lesions, and hepatosplenomegaly that likely is due to hematopoietic neoplasia.

Fig. 6. Histological presentations of subclinical chronic systemic inflammation-associated lesions seen in C57BL/6 mice aged 16–36 months. **A.** Hyperplastic mesenteric milky spot. **B.** Higher magnification of A. The reactive milky spot contains large and small lymphocytes, plasma cells, and Mott cells (arrows). **C.** Low magnification overview of chronic renal lesions. Interstitial lymphoid aggregates (*) and tubular ectasia (arrow) with degeneration, regeneration, necrosis and membranous glomerulonephropathy. **D.** Thickened mesangial matrix (*) and periglomerular fibrosis (arrow) characterize membranous glomerulonephropathy. Glomerular amyloidosis should also be considered. PAS and Congo Red histochemical stains can aid in differentiation. **E.** Chronic adenitis occurs in numerous glands including the exorbital lacrimal gland. **F.** Higher magnification of E. Lymphoplasmacytic inflammation disrupts the gland architecture. Note ectatic duct (*). **G.** Amyloid accumulation in the small intestinal villi. **H.** Higher magnification of G. An accumulation of light pink homogenous extracellular material (amyloid) in the lamina propria widens the villi. **I.** Cross-section of the base of the tongue with poly arteritis nodosa (box and *). Lingual minor salivary glands are indicated (arrow). **J.** Movat's pentachrome staining of lingual artery in I. The affected segment (*) lacks in elastic lamina (thin black line) and the media is expanded by smooth muscle cells. Mild to moderate perivascular chronic inflammatory cells (arrow) and lumena (L) are indicated. Similar necroproliferative arteritis near the inner and middle ear may result in neurological signs (see text for details). **K.** Low power view of lung severely affected by AMP. **L.** Higher magnification of AMP demonstrates the intrahistiocytic crystalline material (*) and dense perivascular and peribronchiolar lymphoplasmacytic inflammation, which is frequently present in severe cases. Hemosiderophage (arrow) and hyalinized respiratory epithelium (arrowheads) are indicated.

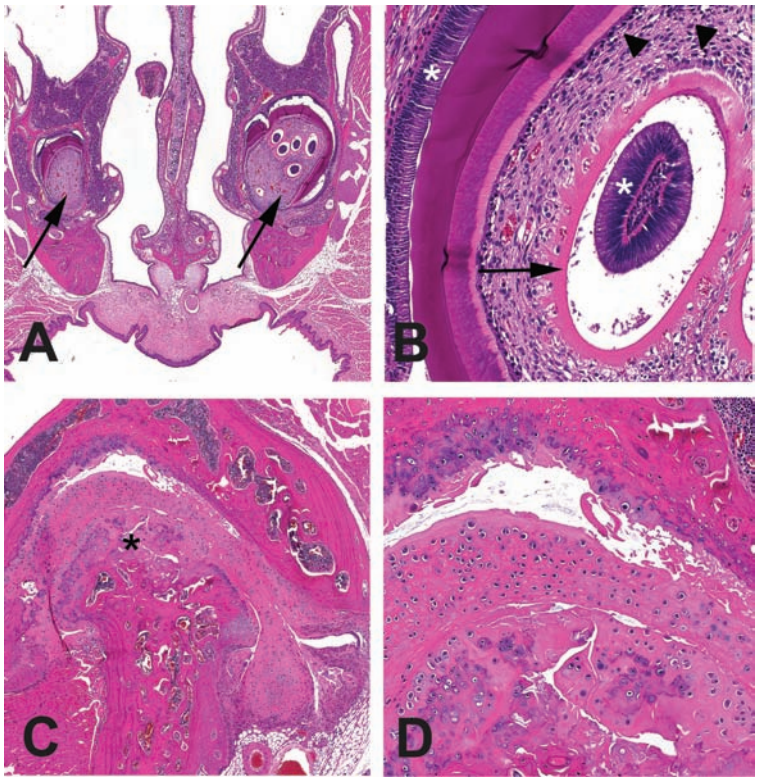

Fig. 7. Subclinical degenerative lesions diagnosed histologically. **A.** Decal cross-section of the nose and incisor roots (arrows) with unilateral multiple immature intrapulpal denticles from a 28-month-old B6 mouse. **B.** Higher magnification of the intrapulpal denticles. Denticles with an unusual presentation of a central column of ameloblasts (*) encircled with clear space, predentin (arrow, pink band) and odontoblasts (arrowhead). Denticles may represent dysplastic tooth development. Normal position of ameloblasts (*) and odontoblasts (arrow) are also indicated. **C.** Osteoarthritis of the temporomandibular joint from the mouse in A with incisor dysplasia. Mandibular condyle is indicated (*). **D.** Higher magnification of boxed region in C. The mandibular condyle and maxillary fossal cartilages are degenerative and irregular. The joint space (*) contains free floating debris and cartilage (joint mice).

Conclusion

In older humans and mice the incidence of chronic disease increases and with it the intensity of clinical care and monitoring. Intensive monitoring of aged mice is needed to prevent undue suffering and loss of valuable data when mice are found dead (18, 19). On the other hand, excessive censoring of mice due to easily observable external non-lethal lesions can impact aging studies (21). A balance is needed and can be achieved via education about the unique appearances and humane care issues associated with geriatric mice (19, 56, 57). Here we have illustrated some of the common clinical, necropsy, and histologic lesions in aged mice to provide a basic introduction into the variety and complexity of age-associated diseases in mice. Necropsy and histopathologic assessments of aged mice coupled with antemortem physiologic testing allows for full characterization of disease onset and patterns, thereby defining frailty and decline in function in aging mouse models. Validation of these models so that they may be better translated to human aging interventions is the goal for the entire biogerontology community of geriatricians, gerontologists, basic scientists, medical and veterinary scientists, and pathologists (5, 6).

Conflict of interest and funding

This work was supported in part by The Seattle Cancer and Aging Program pilot grant (PMT) and NIH grants P01 AG0175 and P01 AG013280 (CPB and PMT).

References

1. Nadon NL. Aged rodents for biogenrontology research. In: Conn PM, ed. Handbook of models for human aging. Amsterdam: Elsevier Academic Press; 2006, pp. 393–401.
2. Boguski MS. Comparative genomics: the mouse that roared. Nature 2002; 420: 515–16.
3. Ladiges W, Van Remmen H, Strong R, Ikeno Y, Treuting P, Rabinovitch P, et al. Lifespan extension in genetically modified mice. Aging Cell 2009; 8: 346–52.
4. Treuting PM, Hopkins HC, Ware CA, Rabinovitch PR, Ladiges WC. Generation of genetically altered mouse models for aging studies. Exp Mol Pathol 2002; 72: 49–55.

Citation: Pathobiology of Aging & Age-related Diseases 2011, **1**: 7202 - DOI: 10.3402/pba.v1i0.7202

5. Kirkland JL, Peterson C. Healthspan, translation, and new outcomes for animal studies of aging. J Gerontol A Biol Sci Med Sci 2009; 64A: 209–12.
6. Tatar M. Can we develop genetically tractable models to assess healthspan (rather than life span) in animal models? J Gerontol A Biol Sci Med Sci 2009; 64A: 161–63.
7. Austad S. Recent advances in vertebrate aging research 2009. Aging Cell 2010; 9: 297–303.
8. Nadon NL, Strong R, Miller RA, Nelson J, Javors M, Sharp ZD, et al. Design of aging intervention studies: the NIA interventions testing program. Age (Dordr) 2008; 30: 187–99.
9. Barthold SW. 'Muromics': genomics from the perspective of the laboratory mouse. Comp Med 2002; 52: 206–23.
10. Kilkenny C, Browne W, Cuthill I, Emerson M, Altman D. Improving bioscience research reporting: the ARRIVE guidelines for reporting animal research. J Pharmacol Pharmacother 2010; 1: 94–9.
11. Maronpot RR, Boorman GA, Gaul BW, eds. Pathology of the mouse. Vienna, IL: Cache River Press; 1999, p. 699.
12. Brayton C, Justice M, Montgomery CA. Evaluating mutant mice: anatomic pathology. Vet Pathol 2001; 38: 1–19.
13. Sundberg JP, Boggess D. Systematic approach to evaluation of mouse mutations. Boca Raton, FL: CRC Press; 2000, p. 199.
14. Maggio-Price L, Treuting P, Zeng W, Tsang M, Bielefeldt-Ohmann H, Iritani BM. Helicobacter infection is required for inflammation and colon cancer in SMAD3-deficient mice. Cancer Res 2006; 66: 828–38.
15. Foltz CJ, Ullman-Cullere M. Guidelines for assessing the health and condition of mice. Lab Anim (NY) 1999; 28: 28–32.
16. Easterly ME, Foltz CJ, Paulus MJ. Body condition scoring: comparing newly trained scorers and micro-computed tomography imaging. Lab Anim (NY) 2001; 30: 46–9.
17. Paster EV, Villines KA, Hickman DL. Endpoints for mouse abdominal tumor models: refinement of current criteria. Comp Med 2009; 59: 234–41.
18. Kennett MJ, Heiderstadt KM. IACUC issues related to animal models of aging. Ilar J 2011; 52: 106–9.
19. Ray MA, Johnston NA, Verhulst S, Trammell RA, Toth LA. Identification of markers for imminent death in mice used in longevity and aging research. J Am Assoc Lab Anim Sci 2010; 49: 282–88.
20. Ullman-Cullere MH, Foltz CJ. Body condition scoring: a rapid and accurate method for assessing health status in mice. Lab Anim Sci 1999; 49: 319–23.
21. Treuting PM, Linford NJ, Knoblaugh SE, Emond MJ, Morton JF, Martin GM, et al. Reduction of age-associated pathology in old mice by overexpression of catalase in mitochondria. J Gerontol A Biol Sci Med Sci 2008; 63: 813–22.
22. Mohr U. International classification of rodent tumors: the mouse. New York: Springer-Verlag; 2001.
23. Lipman RD, Dallal GE, Bronson RT. Lesion biomarkers of aging in B6C3F1 hybrid mice. J Gerontol A Biol Sci Med Sci 1999; 54: B466–77.
24. Yiou R, Delmas V, Carmeliet P, Gherardi RK, Barlovatz-Meimon G, Chopin DK, et al. The pathophysiology of pelvic floor disorders: evidence from a histomorphologic study of the perineum and a mouse model of rectal prolapse. J Anat 2001; 199: 599–607.
25. Boivin GP, Washington K, Yang K, Ward JM, Pretlow TP, Russell R, et al. Pathology of mouse models of intestinal cancer: consensus report and recommendations. Gastroenterology 2003; 124: 762–77.
26. Kastenmayer RJ, Fain MA, Perdue KA. A retrospective study of idiopathic ulcerative dermatitis in mice with a C57BL/6 background. J Am Assoc Lab Anim Sci 2006; 45: 8–12.
27. Andrews AG, Dysko RC, Spilman SC, Kunkel RG, Brammer DW, Johnson KJ. Immune complex vasculitis with secondary ulcerative dermatitis in aged C57BL/6NNia mice. Vet Pathol 1994; 31: 293–300.
28. Dawson DV, Whitmore SP, Bresnahan JF. Genetic control of susceptibility to mite-associated ulcerative dermatitis. Lab Anim Sci 1986; 36: 262–67.
29. Sundberg JP, Taylor D, Lorch G, Miller J, Silva KA, Sundberg BA, et al. Primary follicular dystrophy with scarring dermatitis in C57BL/6 mouse substrains resembles central centrifugal cicatricial alopecia in humans. Vet Pathol 2011; 48: 513–24.
30. Miller R. Principles of animal use in gerontological research. In: Conn PM, ed. Handbook of models for human aging. Amsterdam: Elsevier Academic Press; 2006, pp. 21–31.
31. Percy DH, Barthold SW. Mouse. In: Percy DH, Barthold SW, eds. Pathology of laboratory rodents and rabbits. Ames, IA: Blackwell; 2007, pp. 3–124.
32. Wolf N, Galecki A, Lipman R, Chen S, Smith-Wheelock M, Burke D, et al. Quantitative trait locus mapping for age-related cataract severity and synechia prevalence using four-way cross mice. Invest Ophthalmol Vis Sci 2004; 45: 1922–29.
33. Wolf N, Penn P, Pendergrass W, Van Remmen H, Bartke A, Rabinovitch P, et al. Age-related cataract progression in five mouse models for anti-oxidant protection or hormonal influence. Exp Eye Res 2005; 81: 276–85.
34. Finch CE, Girgis FG. Enlarged seminal vesicles of senescent C57BL-6J mice. J Gerontol 1974; 29: 134–38.
35. Brayton C. Spontaneous diseases in commonly used inbred mouse strains. In: Fox JG, ed. The mouse in biomedical research. 2nd ed., Vol. 3. Amsterdam: Elsevier, Academic Press; 2006, pp. 623–718.
36. Ward J, Anver M, Mahler W, Devor-Henneman T. Pathology of mice commonly used in genetic engineering: C57Bl/6; 129; B6, 129; and FVB/N. In: Ward JM, Maronpot RR, Sundberg JP, Frederickson RM, eds. Pathology of genetically engineered mice. Ames, IA: Iowa State Press; 2000, pp. 161–79.
37. Turturro A, Duffy P, Hass B, Kodell R, Hart R. Survival characteristics and age-adjusted disease incidences in C57BL/6 mice fed a commonly used cereal-based diet modulated by dietary restriction. J Gerontol A Biol Sci Med Sci 2002; 57: B379–89.
38. Hao X, Fredrickson TN, Chattopadhyay SK, Han W, Qi CF, Wang Z, et al. The histopathologic and molecular basis for the diagnosis of histiocytic sarcoma and histiocyte-associated lymphoma of mice. Vet Pathol 2010; 47: 434–45.
39. Morse HC III, Anver MR, Fredrickson TN, Haines DC, Harris AW, Harris NL, et al; Hematopathology subcommittee of the Mouse Models of Human Cancers Consortium. Bethesda proposals for classification of lymphoid neoplasms in mice. Blood 2002; 100: 246–58.
40. Kogan SC, Ward JM, Anver MR, Berman JJ, Brayton C, Cardiff RD, et al; Hematopathology subcommittee of the mouse models of human cancers consortium. Bethesda proposals for classification of nonlymphoid hematopoietic neoplasms in mice. Blood 2002; 100: 238–45.
41. Frith CH, Ward JM, Harleman JH, Stromberg PC, Halm S, Inoue T, et al. Hematopoietic system. In: Mohr U, ed. International classification of rodent tumors. Part II. The mouse. New York: Springer: WHO-International Agency for Research on Cancer; 2001, pp. 417–51.
42. Seely JC. Kidney. In: Maronpot RR, Boorman GA, Gaul BW, eds. Pathology of the mouse. Vienna, IL: Cache River Press; 1999, pp. 207–34.
43. Haines DC, Chattopadhyay S, Ward JM. Pathology of aging B6/129 mice. Toxicol Pathol 2001; 29: 653–61.

44. Gaillard ET. Ureter, bladder and urethra. In: Maronpot RR, Boorman GA, Gaul BW, eds. Pathology of the mouse. Vienna, IL: Cache River Press; 1999, pp. 235–58.
45. Alpers CE. The Kidney. In: Robbins SL, Kumar V, Cotran RS, eds. Robbins and Cotran pathologic basis of disease. Philadelphia, PA: Saunders/Elsevier; 2010, pp. 905–70.
46. Mathieson PW, Qasim FJ, Esnault VL, Oliveira DB. Animal models of systemic vasculitis. J Autoimmun 1993; 6: 251–64.
47. Stone JH. The systemic vasculitides. In: Cecil RL, Goldman L, Ausiello DA, eds. Cecil medicine. Philadelphia, PA: Saunders/Elsevier; 2008, pp. 2049–58.
48. Krabbe KS, Pedersen M, Bruunsgaard H. Inflammatory mediators in the elderly. Exp Gerontol 2004; 39: 687–99.
49. Bruunsgaard H, Pedersen BK. Age-related inflammatory cytokines and disease. Immunol Allergy Clin North Am 2003; 23: 15–39.
50. Rangel-Moreno J, Moyron-Quiroz JE, Carragher DM, Kusser K, Hartson L, Moquin A, et al. Omental milky spots develop in the absence of lymphoid tissue-inducer cells and support B and T cell responses to peritoneal antigens. Immunity 2009; 30: 731–43.
51. Ward JM, Yoon M, Anver MR, Haines DC, Kudo G, Gonzalez FJ, et al. Hyalinosis and Ym1/Ym2 gene expression in the stomach and respiratory tract of 129S4/SvJae and wild-type and CYP1A2-null B6, 129 mice. Am J Pathol 2001; 158: 323–32.
52. Murray AB, Luz A. Acidophilic macrophage pneumonia in laboratory mice. Vet Pathol 1990; 27: 274–81.
53. Hoenerhoff MJ, Starost MF, Ward JM. Eosinophilic crystalline pneumonia as a major cause of death in 129S4/SvJae mice. Vet Pathol 2006; 43: 682–88.
54. Long PH, Herbert RA. Epithelial-induced intrapulpal denticles in B6C3F1 mice. Toxicolog Pathol 2002; 30: 744–48.
55. Long PH, Leininger JR. Bones, Joints, and Synovia. In: Maronpot RR, Boorman GA, Gaul BW, eds. Pathology of the mouse. Vienna, IL: Cache River Press; 1999, pp. 645–73.
56. Clough G. Suggested guidelines for the housing and husbandry of rodents for aging studies. Neurobiol Aging 1991; 12: 653–58.
57. Nadon NL. Maintaining aged rodents for biogerontology research. Lab Anim (NY) 2004; 33: 36–41.
58. Quinby FL. Clinical chemistry of the laboratory mouse. In: Fox JG, ed. The mouse in biomedical research. 2nd ed., Vol. 3. Amsterdam: Elsevier, Academic Press; 2007, pp. 171–216.
59. Suckow MA, Danneman P, Brayton PC. The laboratory mouse. The Laboratory animal pocket reference series. Boca Raton, FL: CRC Press; 2001.

***Piper M. Treuting**
Department of Comparative Medicine & Histology and Imaging Core
School of Medicine
University of Washington
T140 Health Science Center
Box 357190
Seattle, WA 98195-7190
USA
Tel: 206-616-6725
Fax: 206-685-3006
Email: treuting@uw.edu

Citation: Pathobiology of Aging & Age-related Diseases 2011, **1**: 7202 - DOI: 10.3402/pba.v1i0.7202